Double Tee Flange Connections – Analytical Evaluation

Clay Naito[1], Andy Osborn[2], Eisa Rahmani[3], Robin Hendricks[4]

Introduction and Background

For over 50 years, prestressed concrete double tee members have been the component of choice for parking structures throughout the United States. The double tee members are laid side by side and typically span approximately 60 ft. The 60 ft span is desirable because it provides a column free span over two drive aisle lanes flanked on both sides by parking stalls.

Double tee flanges, which were primarily 8 ft. wide in the beginning, have increased incrementally to a width of 16 ft., with the most common current width nationwide being 12 ft. The properties of a typical 12 ft. wide by 30 in. deep, pretopped double tee, suitable to span 60 ft. are indicated in Figure 1.

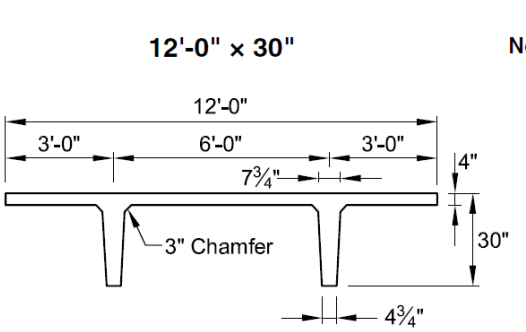

Section Properties

	Normalweight	Lightweight
A	928 in.²	928 in.²
I	59,997 in.⁴	59,997 in.⁴
y_b	22.94 in.	22.94 in.
y_t	7.06 in.	7.06 in.
S_b	2615 in.³	2615 in.³
S_t	8498 in.³	8498 in.³
wt	967 lb/ft	741 lb/ft
DL	81 lb/ft²	62 lb/ft²
V/S	2.30 in.	2.30 in.

Figure 1: 12DT30 section details

Initially, double tee top flanges were 2 in. thick. Steel angles, or plates with reinforcing bar anchorages or bent rebar were embedded at 5 to 10 ft intervals along the flange edges. The embed plates of adjacent tees were connected via welded faceplates (Figure 2). Then a 2 in. to 3 in. thick cast-in-place concrete topping, reinforced with wire mesh, was poured over the entire deck, creating an overall flange thickness of 4 to 5 in. This system was the only one shown in PCI Design Handbook Editions 1, 2, and 3. Joints were formed in the concrete topping using a grooving tool, centered over the double tee joints to allow relief cracks to form at those locations. The joints were filled with sealant after the concrete topping cured. Continuity was provided between double tees by the weld plates and the reinforced topping.

The development of an integral 4 in. thick flange began in the late 1970's, at which time it was referred to as "untopped". The current terminology, "pretopped" double tee, first appeared in the PCI Handbook, 4th

1 Professor, Department of Civil Engineering, Lehigh University, 13 E Packer Ave, Bethlehem, PA 18015, Email: cjn3@lehigh.edu
2 Senior Principal, Wiss Janney Elstner Associates, Inc., 311 Summer Street, Suite 300, Boston, MA 02210, Email: aosborn@wje.com
3 Associate II, Wiss, Janney, Elstner Associates, Inc., 330 Pfingsten Road, Northbrook, IL 60062.
4 Research Engineer, ATLSS Center, Lehigh University, 117 ATLSS Dr., Bethlehem, PA 18015.

Edition, published in 1992. The use of pretopped double tees is commonplace in most of the United States today (California, Texas and Arizona still use field topped tees). Cast-in-place, reinforced concrete toppings, sometimes referred to as pour strips, are commonly utilized only at the ends of the double tees to provide an area for chord reinforcement as well as smooth transitions and continuity over inverted T beams. Dry systems comprised of welded connections, which eliminates the wet joints, have also been used for decades in some regions with low seismic risk.

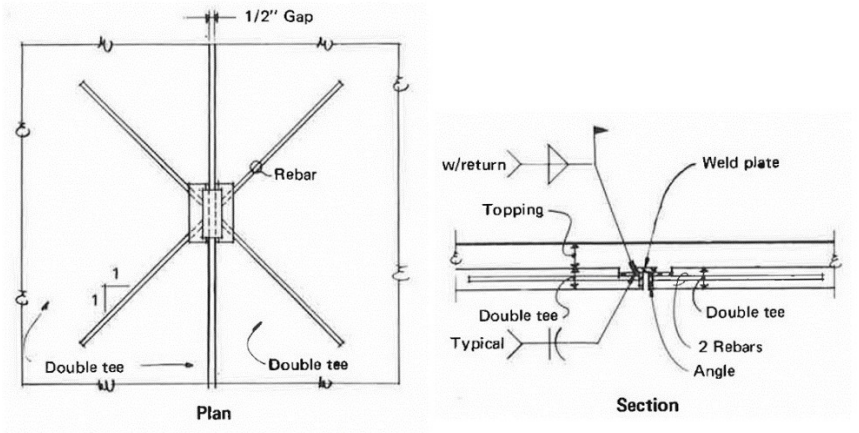

Figure 2: Flange to flange connections for 2 in. flange thickness covered by cast in place topping (from PCI 1971)

To provide lateral continuity between pretopped double tees, away from ends, weld plate connections have typically been used. For pretopped double tees, earlier weld plate connections were plant-fabricated plates with headed studs, deformed bar anchors, or welded rebar for anchorage into the flange. The double tees were joined using a round bar or rectangular slug, also called a jumper plate or an erection plate, welded to the embedded flat plates (Figure 3). Starting around 1976, proprietary connection hardware began to be marketed and sold in the US (Figure 4). The original proprietary connections were made from galvanized mild steel. Increasingly, in northern climates subject to road salts, the connections have been fabricated from stainless steel. Three common manufactured connectors used in the US today are illustrated in Figure 5. They all have similarities in that they all consist of a faceplate with integral wings that are embedded in the concrete. Currently, the most common type of jumper plate is a 3/8 in. wide by 2 ½ in. to 3 ½ in. long plate. Round slugs of similar dimensions are sometimes used instead of plates. Plate widths and slug diameters are adjusted to accommodate variable joint gaps between double tees, but are typically about 1 in. wide. Connections are usually spaced 5ft. to 8 ft. on center with closer spacings sometimes used at the mid-span of the double tees. After welding, the flange to flange gap is filled with sealant to prevent water leakage between the double tee joints to spaces below.

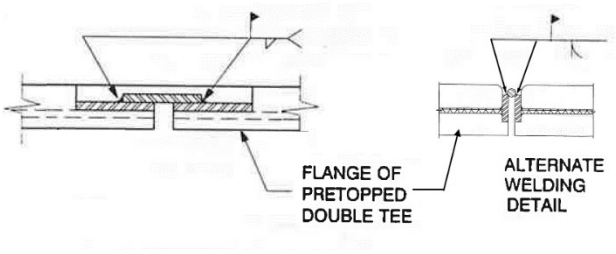

Figure 3: Typical "pretopped" flange to flange connection details from PCI Design Handbook, 5th Edition, 1998.

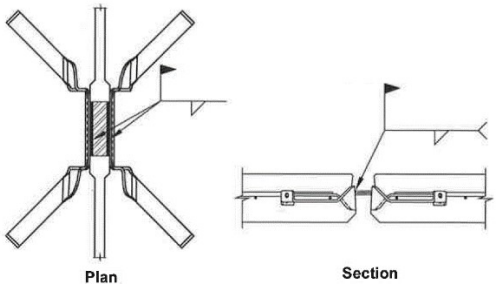

Figure 4: Proprietary "pretopped" flange to flange connection detail from PCI Design Handbook, 6th Edition, 2002.

Manufacturer 1 Manufacturer 2 Manufacturer 3

Figure 5: Proprietary connectors currently available in the marketplace

A typical assembly of two flange to flange connectors with a welded jumper plate between is presented in Figure 6 (concrete flanges not shown for clarity). Standard details for all three connectors are presented in Figure 7. In all cases, a fillet weld is used to join the jumper plate to the embedment face plate. These fillet welds are typically 1/4 in. to 3/8 in. in size and extend for the full length of the jumper plates.

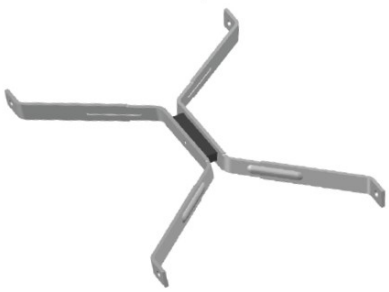

Figure 6: Typical welded assembly consisting of two winged connectors (Manufacturer 2 shown) and jumper plate. Concrete not shown for clarity

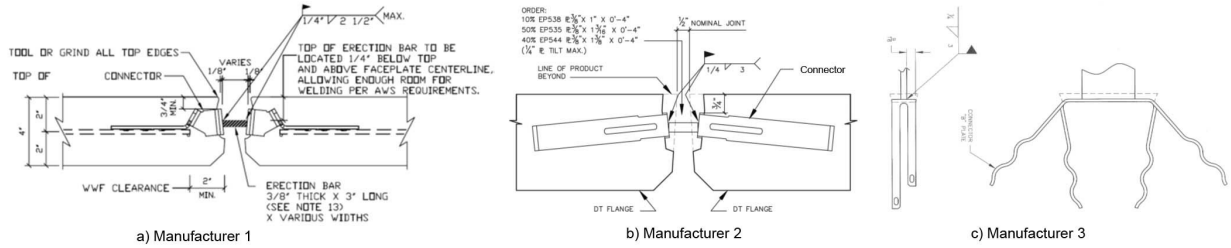

Figure 7: Standard details published by three connector manufacturers

Recently Raised Concerns

Recently, concerns have been raised regarding the repeated transverse loading of these welded flange connections in parking garages. An article has been written by a consultant warning of the potential for

fatigue cracking and brittle fracture of welds due to repeated loading from automobiles. The mechanism of cyclic loading arises from the passage of vehicles over the joints. As illustrated in Figure 8, as the wheel approaches from the left the connector plates bend counterclockwise, tending to cause positive flexure on the left weld and negative flexure on the right weld. As the wheel passes across the joint, the connector plates rotate in the clockwise direction and the stresses reverse. Only a portion of the wheel load is transferred across the joint. The majority of the wheel load is transferred to the double tee end supports. Keenan shows examples of welds with demonstrated fatigue striations and presents analysis purported to justify the concerns raised in the article.

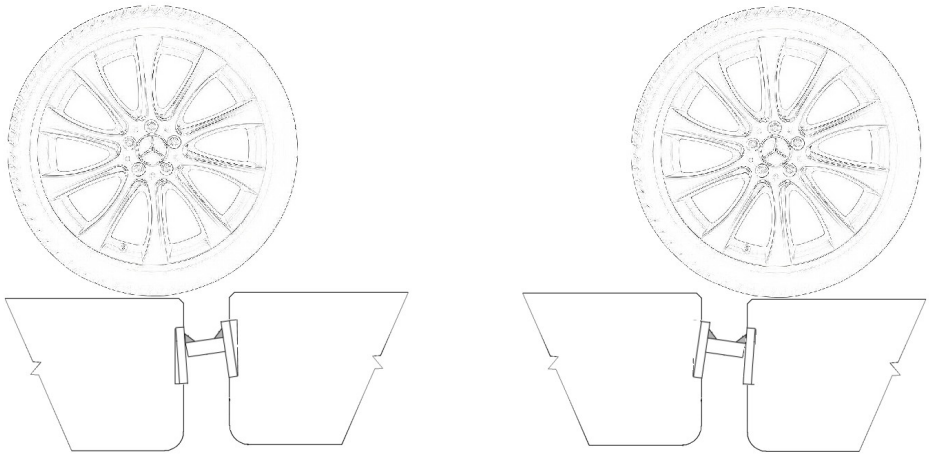

Figure 8: Deformations on flange-to-flange connection due to wheel loads

A Task Group was created at the Precast/Prestressed Concrete Institute (PCI) to investigate the concerns raised by Keenan. An informal poll of producers, who had been fabricating and erecting double tee parking garages for decades, indicated that weld fractures were uncommon and when they occurred, were usually associated with atypical joint conditions or a lack of maintenance. No widespread reports of fatigue problems had been received. The Task Group also inquired of the experiences of consulting firms that commonly perform inspections and evaluations of precast parking garages. The group was told that problems with flange to flange joints do occur, but are due a wide variety of issues.

As previously mentioned, under vehicle loading, connections are subject to vertical deformation and force. The manner in which the forces are transferred through the connection assembly in part determines the stress levels in the weld. One approach is to assume that the jumper plate undergoes flexure and that the connection faceplates act as fixed boundaries as shown in Figure 9a. An alternate approach is to account for the flexibility provided by the faceplates of the embedded connectors, which would reduce jumper plate flexure and weld stresses (see Figure 9b). Based upon the concept that faceplate flexure would reduce weld stresses, the Task Group determined that studies would need to be conducted to ascertain actual connection behavior when subject to transverse loads.

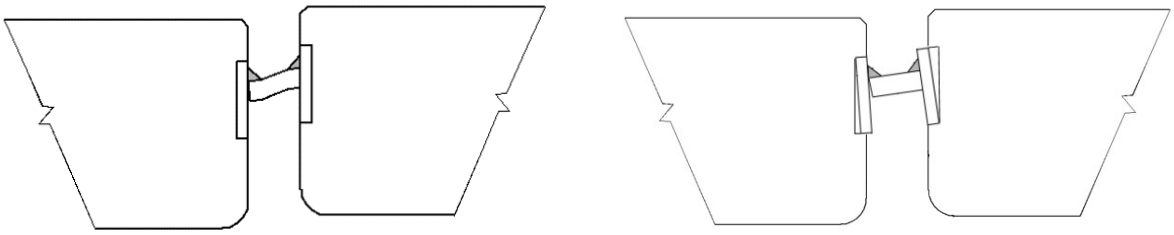

a) Assumption 1 - deformation within jumper plate, face plates are fixed

b) Assumption 2 – reduced deformation of jumper plate, face plates rotate

Figure 9: Flexibility assumptions for connection assembly

As recommended by the Task Group, PCI has undertaken several parallel research projects designed to advance the understanding of the loading and behavior of welded double tee flange connections. Two parallel efforts were undertaken: one project (Lucier et al.) describes full scale testing and test results. The other project, the subject of this paper, was analysis oriented. This paper presents work and findings to date pertaining to the analytical work, in addition to background information. This paper also reports briefly on field evaluation of a garage structure and component tests.

Case Study

A recent assignment by one of the authors pertained to an investigation of connection failures in a parking garage built in 2008. Two connections were extracted from the structure, one with a completely failed weld and the other still welded (Figure 10). The weld failures occurred primarily on ramps in high traffic areas. Certain features of failed welds were recorded as follows:

- The weld size was smaller than specified (0.15 in. instead of 0.25 in.);
- The weld was deeper below the surface than specified (1.25 in. instead of 0.75 in. max)
- The plate was wider than specified (1.5 in. instead of 1.0 in.)
- The welds generally extended to the ends of the 3-1/2 in. plate instead of terminating 1/4 in. from each end as required by the shop drawings
- At the failed weld, there did not appear to be adequate weld penetration into the base metal (Figure 11);
- At the intact welds, there were partial depth cracks observed at both ends (Figure 12).

Figure 10: Flange connection hardware extracted from parking garage

Figure 11: Inadequate weld to base metal penetration observed at failed weld location

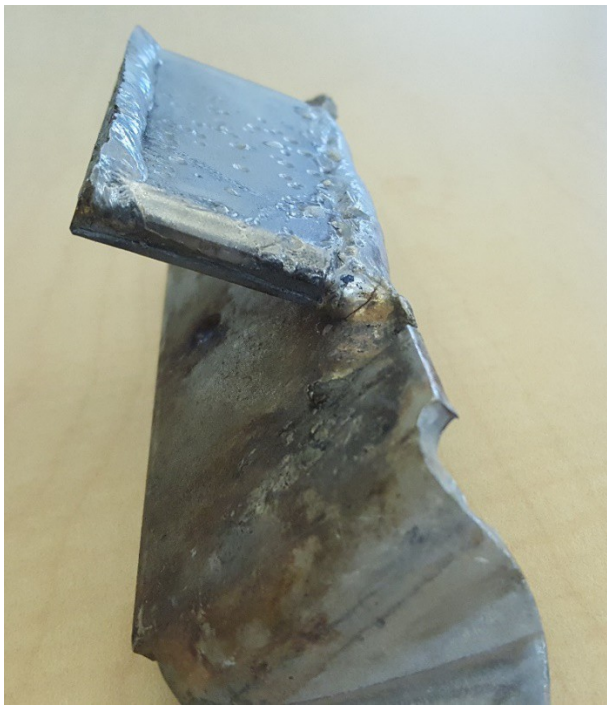

Figure 12: Crack at end of intact weld

Vehicle Loads

Vehicle loads in parking structures are defined by ASCE 7 Minimum Design Loads for Buildings and Other Structures. The ASCE 7 load standard states that the design point load for garages restricted to passenger vehicles accommodating not more than nine passengers shall be designed for 3,000 lb. (13.35 kN) acting on an area of 4.5 in. by 4.5 in. This static load represents a potential vehicle jacking load and is placed such that it generates the worst case effect. This load typically controls the strength design of connections for vertical shear transfer between double tees.

Since the occurrence of such a load is low, it does not represent a fatigue concern. To properly assess fatigue resistance of connections within a double tee floor system the magnitude and number of typical loads should be considered. Under conventional vehicular loading, point loads are considerably lower than the 3000 lb. ASCE 7 static load. Wen and Yeo examined vehicle load distributions in U.S. parking garages through a survey of nine structures. The study found that the average vehicle weight was 3400 lbs. with loads as high as 8750 lbs. and as low as 1750 lbs. The distribution is recreated in Figure 13. Since the intensity of cyclic loading varies with vehicle size the Wen and Yeo distribution must be used with a cumulative damage model such as Miner's rule to evaluate susceptibility to fatigue failure. Data on average vehicle weight by vehicle model year has been collated by the Environmental Protection Agency. The EPA study indicates that the average car and truck curb weight plus 300 lbs. occupant load increased only 4% since the work of Wen and Yeo was conducted (car increase 3411 to 3617 lbs. and truck increase 4543 to 4680 lbs. from 2001 to 2015). Consequently, the distributions and averages developed for parking

structures in 2001 are still applicable at the time of this writing. Keenan assumed an average vehicle load of 4250 lbs distributed equally to front and rear axles. This value is higher than the 2015 average vehicle curb weight plus 300 lbs. noted by EPA for cars, 3617 lbs., or all vehicle types, 4035 lbs.

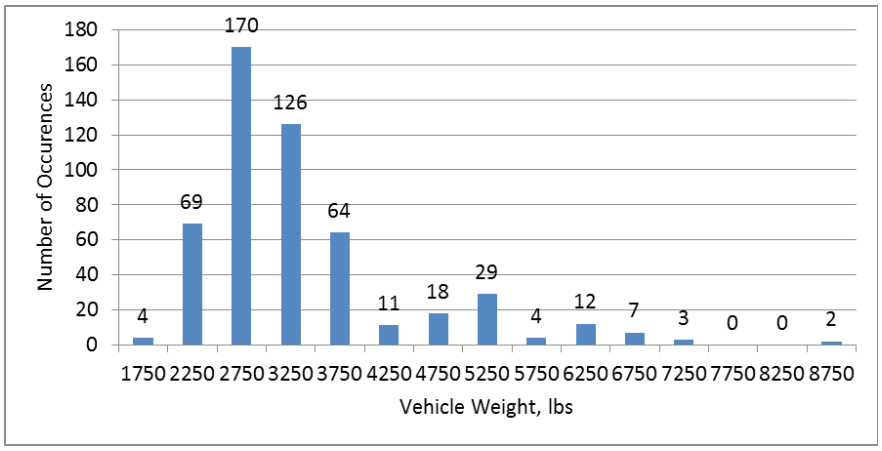

Figure 13: Vehicle distribution (Adopted from Wen and Yeo)

Fatigue demands on parking garages can be determined by examination of the vehicle loading and the configuration of the double tee flange-to-flange connection. A plan view of a conventional double tee is illustrated in Figure 14. The flange to flange connection locations are illustrated by circles and a vehicle is included to provide scale.

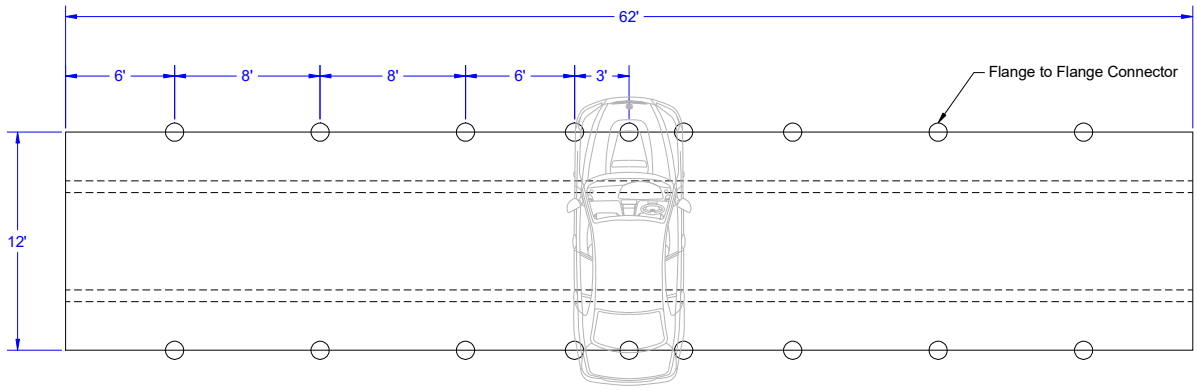

Figure 14: Flange to flange connections and vehicle location on DT panel

Number of Potential Fatigue Cycles

For a double tee located at the entry of a garage the following loading conditions are postulated:

Entry Location: 500 cars x 2 passes x 2 axles = 2000 cycles/day

As distance from the entryway of the garage increases, or as one moves from the drive lanes to the parking stalls, the number of cycles decreases. For example, a double tee located on the top floor of a parking garage with a 1st floor entrance would only see the vehicles that make it to the top floor.

Roof or parking stall location: 20 cars x 2 passes x 2 axles = 80 cycles/day

The traffic in a parking structure varies considerably based on the customers being served. For example, a residential garage would likely be utilized 365 days a year while a garage that serves a commercial area may only be fully occupied a fraction of the year. Residential and office building garages may see each occupant exit and enter only once per day while garages at shopping centers may see numerous entrances and exits per day for each parking stall. Consequently, over a 30-year life the cyclic loading on the flange connections can vary considerably based on the usage of the structure and the location of connection within the garage. However, for the example above, the following estimates of lifetime load cycles are calculated.

Entry Location Heavy Usage: 2000 cycles/day x 365 days/year x 30 years = 21.8 million cycles

Roof Location or parking stall, Low Usage: 80 cycles /day x 120 days/year x 30 years = 0.28 million cycles

Keenan presents a sample calculation that estimates the lifetime loading of a welded connection could approach 21 million cycles. That number could be correct as described above, but only for a select number of garages and selected locations within those garages.

Preliminary Structural Analysis of Double Tees and their Flange to Flange Connections

Preliminary analysis was performed using a finite element model of five, typical 60 ft span, 12 ft wide double tee beams. Connector face plate separation between beams was set at 1 in. Flange connection assemblies were modelled as link beams spaced at 5 ft. on center. Typical flange connection jumper plates were 3/8 in. x 1 in. by 3 in. with 1/4 in. x 3 in. fillet welds on each side welded to the face of the connector. If the ends of the jumper plate are assumed to be fixed at both ends, stiffness can be estimated based on the cantilever formula: . With elastic modulus, E, set as 29,000,000 psi, moment of inertia, I, $(0.375)^3$ x 3 / 12 = 0.013 $in.^4$, and plate width, L, 1 in., the stiffness, K, becomes 1,130,000 lbs./in. In reality, the face plate of the connector rotates under load. Component testing discussed below suggests that a reasonable first estimate of connection stiffness is around 90,000 lbs./in.

To create a jumper plate with a stiffness of 90,000 lbs./in., the connection was modeled as a beam with a thickness of 0.14 in. and a width of 3 in. A beam element was used with a section modulus of 0.03 $in.^2$ to model the section modulus of a 1/4 in. by 3 in. long weld. Two 1063 lb. wheel loads spaced 5 ft. apart were placed adjacent to two midspan connections representing the axle load assumed by Keenan. The overall model is shown in Figure 15 and the detail at a flange to flange joint is shown in Figure 16.

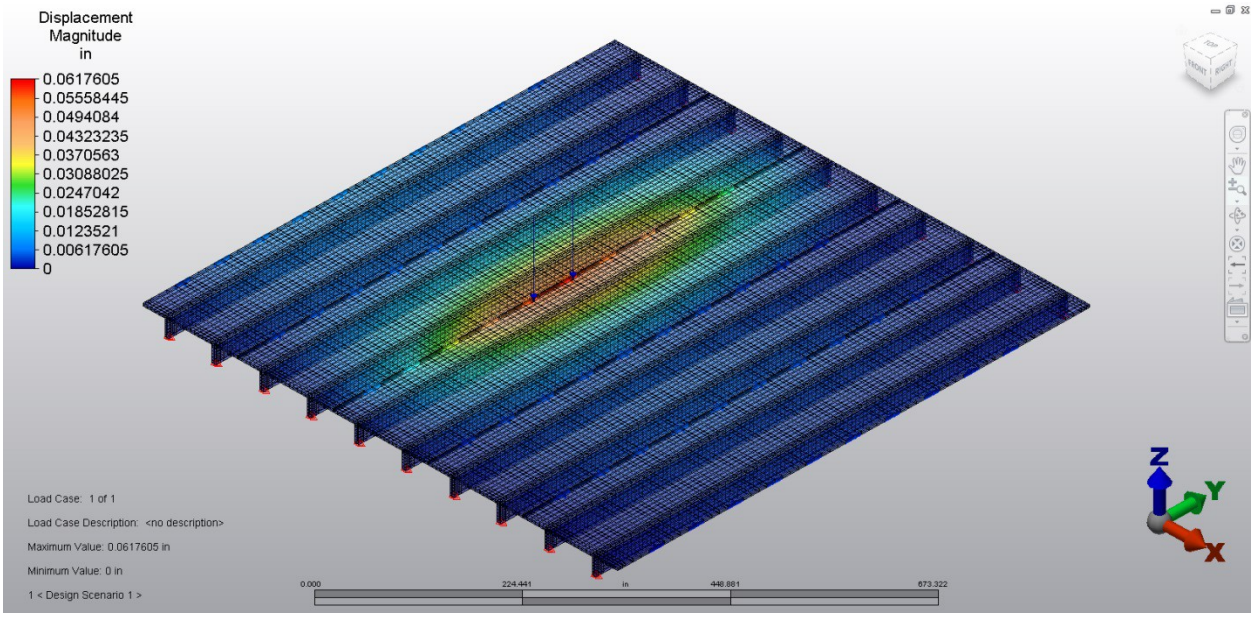

Figure 15: Deflected model of five Double Tee beams supporting an axle load (2 wheels) of 2125 lbs

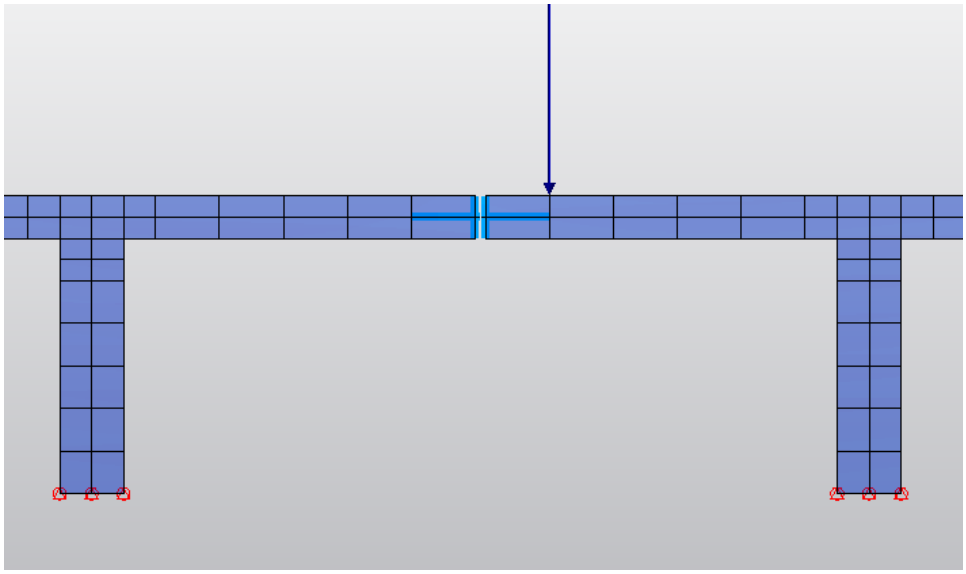

Figure 16: Undeflected model, showing beam elements used to mimic flange to flange connections

Preliminary Analysis Results

The model predicted a maximum live load deflection of 0.062 in. and a differential deflection from one side of the joint to the other of 0.004 in. The compressive bending stress in the weld adjacent to the wheel load was predicted to be -6507 psi (Figure 17), which equates to a bending moment of 180 in.-lbs. The corresponding calculated shear force in the jumper plate was 180 in.-lbs. / 0.5 in. = 360 lbs. As the wheel passes over the joint, the stress becomes tensile (+5543 psi) such that the total stress range on either weld was 12,050 psi. The calculated maximum shear was 110% greater than that calculated by Keenan and the weld stress range was 9% greater.

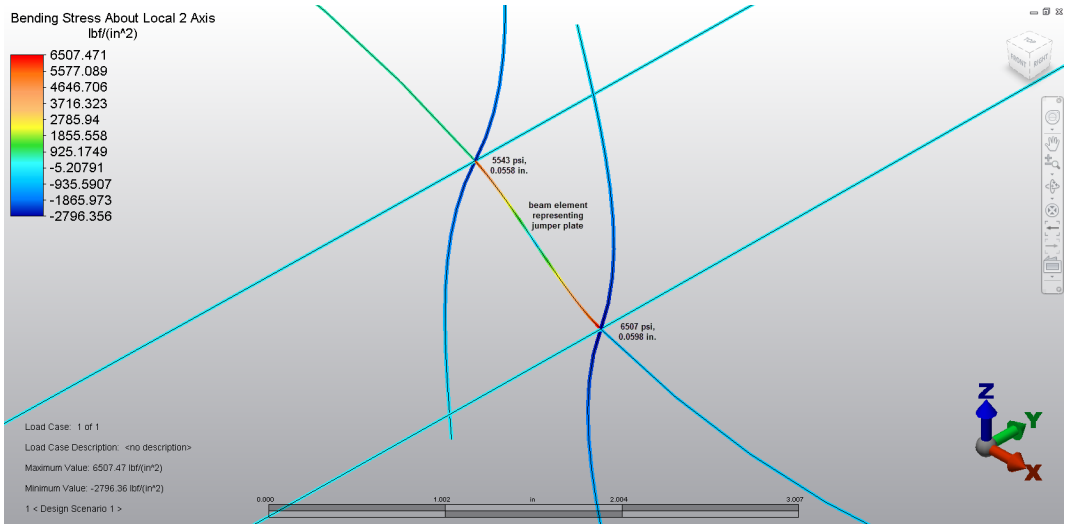

Figure 17: Beam element simulating connector plate showing bending stresses and displacements at a loaded joint

The stresses on the flange connection welds and shear forces transferred by the jumper plate vary along the span of the double tee. As illustrated in Figure 18, when a vehicle is centered along an edge (point loads at 300 in. and 360 in.), the welds at midspan will be subjected to the highest stresses and shear forces while welds located away from the wheel load experience lower stresses and shear forces. The sum of shear forces is 1002 lbs. indicating that 47% of the two wheel loads transfers laterally across the joint and 53% is transferred to the loaded beam bearings. If the wheels are positioned between connectors, the maximum shear force in any one connector decreases.

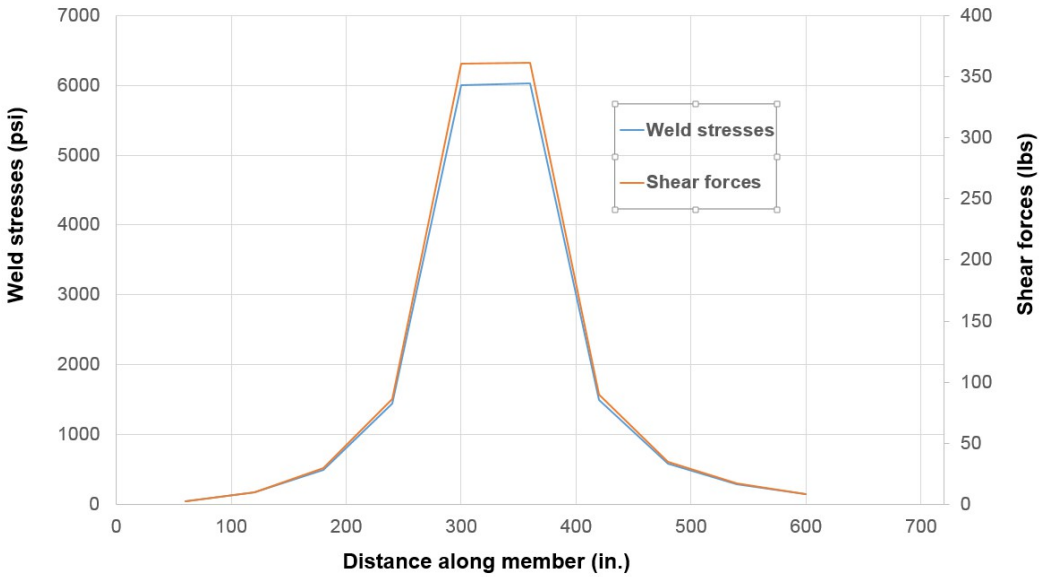

Figure 18: Distribution of weld stresses and shear forces along double tee joint from simplified analytical model, two concentrated wheel loads of 1063 lbs. each

Based on these results, the stresses appeared to be high enough to raise concerns regarding fatigue of the jumper plate welds, and further investigation was recommended by the Task Group. The additional investigation recommended including measurements of flange to flange connection differential displacements under load at several parking garages, literature review, component tests of single connection weld assemblies (three brands of connectors), and tests of full sized double tee beams joined using two brands of connectors.

In-Situ Testing

Tests were performed at two garages as reported in Lucier et al[8]. In these tests, axle loads were 20 to 35% greater than assumed in the analysis described above. Differential displacements across the joints for both in-situ tests averaged 0.014 in.

Component Tests

A significant number of component tests have been conducted on flange to flange connections. Early testing was conducted by Venuti, Spencer and Neille, and Aswad on non-proprietary connections and continued on manufactured connections by Pincheira et al., Oliva, WJE, Shaikh and Fiele, and Naito et al. Testing consisted of in-plane shear and tension and out-of-plane shear forces across the joint. A large number of the studies are summarized in Ren and Naito. A few of the recent studies focused on out-of-plane load testing of Manufacture 1, 2 and 3 connections are discussed.

Proprietary Tests for Manufacturer 1 at University of Wisconsin

These tests involved small panels of concrete 4 ft by 4 ft by 4 in. thick with embedment hardware on all four faces. Tests for vertical shear were performed in 2000, 2002, 2004, and 2010. Connectors were varied over the years, but all had the same general shape and dimensions. Test loads were applied via a vertical plate welded to a 1 in. by 4 in. wide jumper plate. The vertical plate was restrained against rotation. Both 1/4 in. and 3/8 in. thick jumper plates were used. Welds were always specified to be 1/4 in. size by 3 in. long. Tests were conducted with upward and downward directed loads. Displacements were measured at the load point relative to the face plate of the connector. Overall, displacements were linear up to at least 1000 lbs. Displacement at 500 lbs. ranged from 0.001 in. to 0.005 in., implying a joint stiffness of 100 to 500 kip/in.

Proprietary Tests for Manufacturer 2 at Lehigh University

These tests involved subassembly tests of connections embedded in concrete measuring 4 ft by 4 ft by 4 in. thick. Connectors were embedded at the manufacturer recommended locations on all four faces. Tests were performed by Naito and Hendricks and Ren and Naito. The test series was conducted to determine the out-of-plane shear force capacity of the connection. Consequently, only one side of the connection was tested. This included a loading arm rigidly attached to a jumper plate welded to the embedded connector. The loading arm was not restrained against rotation. The average elastic stiffness was 24.6

kip/in for the 2008 tests and 31.9 kips/in. for the 2010 tests. These tests consisted of a 4 in. wide jumper plate. This is much wider than traditional jumper plates which range from 0.75 to 1.5 in. in width for a whole connection. The large width may have contributed to a lower apparent stiffness.

Proprietary Tests for Manufacturers 1 and 2 at NCSU

These tests were performed in 2012. The test setup included two double tees side by side with Manufacturer 1 connectors. Test results are summarized in Botros et al. Displacements were measured only for a few of the tests. Test 2B was most relevant to the current study wherein a 0.015 in. differential deflection was measured at a midspan load of 500 lbs., implying a connection assembly stiffness of about 33.0 kip/in.

Small Specimen Tests at Lehigh University.

Twelve tests were performed as part of the current PCI research in DT flange connectors by Naito and Hendricks. These tests involved small panels of concrete 4 ft. by 4 ft. by 4 in. thick with embedment hardware on all four faces. Weld sizes were 1/4 in. Centroid of load was 1 in. from the face of the embed plate. Loads were applied in the upward and downward directions. Three connector manufacturers were represented (Figure 19). For each manufacturer, both mild steel and stainless steel versions of their connectors were tested.

Figure 19: Forms for component panels tested at Lehigh University.

Displacements were measured in line with the load application. The rotation of the jumper plate was monitored as were strain gages applied to welds, jumper plate, and face plate. Test setup details are presented in Figure 20 to Figure 22. The loading block was not restrained against rotation.

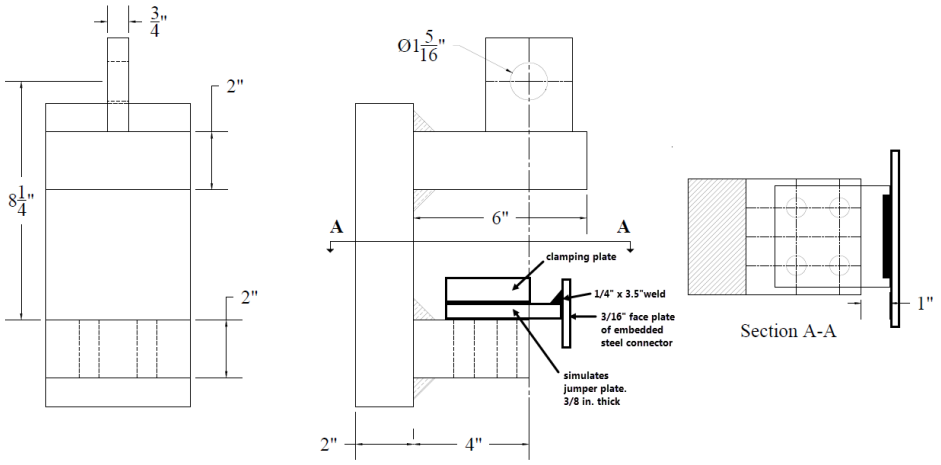

Figure 20: Loading apparatus and specimen connector details

Figure 21: Typical "jumper plate"

Figure 22: Assembly ready to test

The connectors were tested in the upward and downward direction relative to vertical shear on the faceplate. The approximate stiffness of the connectors up to a load level of 600 lbs. is summarized for both the stainless steel and carbon steel connectors in Table 1. An average connector stiffness for the twelve tested connectors was 32.8 kips/in. It is important to note that since the tests were conducted on single sided connectors the results do not represent the combined behavior of the entire welded connection. The results should be used to compare the relative stiffness of the various connectors available and to verify numerical models which can be used to examine the entire connection.

Table 1: Single-sided connection stiffness (kips/in.)

	Carbon Up	Carbon Down	Stainless Up	Stainless Down
Manufacturer 1	23.1	42.9	37.5	23.1
Manufacturer 2	11.8	22.2	30.0	15.0
Manufacturer 3	34.3	40.0	64.0	50.0

Full Scale Tests at Tindall Corporation in Petersburg, VA

To better refine analytical models, full scale tests were conducted. In these tests, three double tee beams were fabricated and positioned side by side. The connectors along one joint between double tees were from Manufacturer 1. The connectors along the other joint were from Manufacturer 2. Details of the test

setup and results are presented in detail in Lucier et al.. Data gleaned from the tests was used to develop and refine detailed finite element models. Figure 23 is excerpted from Lucier et al.[8] for comparison of measured and predicted stress ranges.

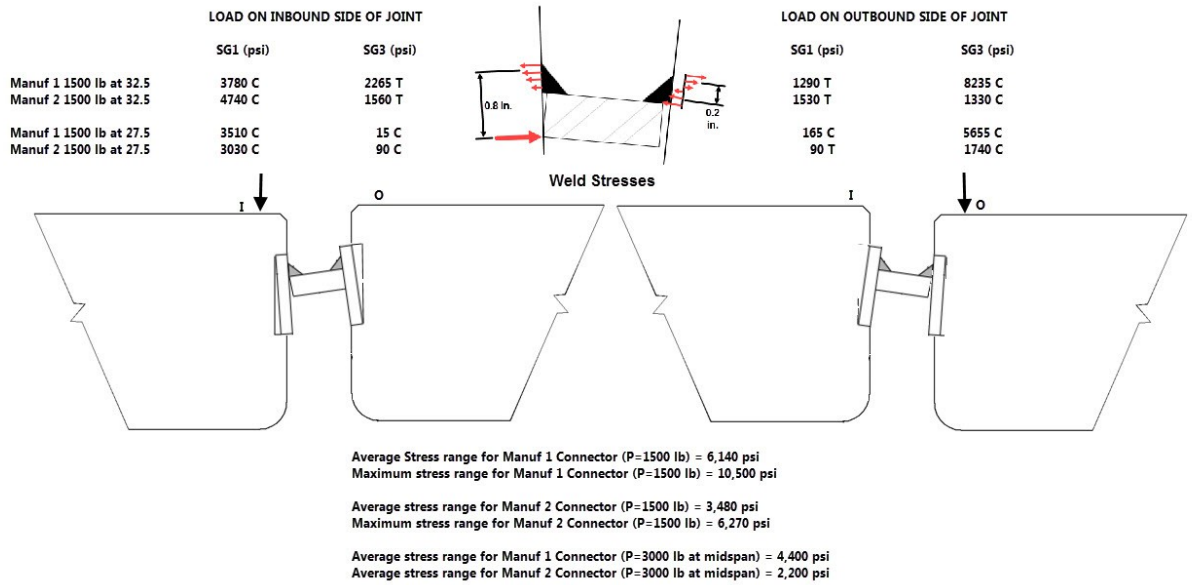

Figure 23: Summary of weld stresses at connectors near midspan of the test specimen. Stress reported at 1500 lbs load is determined from the microstrain at 3000 lb load x 30 (MOE) / 2 (from Lucier et al.)

Refined Finite Element Analyses

The initial models reported earlier appeared to predict double tee displacements fairly well, including differential displacements between adjacent double tees. However, realistic characterization of the connection behavior was not captured. Initial FEA studies of these weldments indicated that there was a significant strain gradient in the welds, face plates, and jumper plates that vary along the length of these elements. A refined model was needed to better understand the distribution of these stresses and to compare them to the measured data. The final baseline model of the three double tee beams and their connections was developed and analyzed in ABAQUS. Altogether, 2.7 million elements were used to properly define the test beams and connection assemblies. Meshing of two different connectors, the jumper plates, and welds are shown in Figure 24. Assigned dimensions for the base model, meant to reflect the as-designed test beams and connections, is presented in Figure 25. The model was developed assuming that one edge of the face plate would bear against the face of the concrete flange. Contact elements were used to form that model. Similarly, contact elements were used to define the interaction of the jumper plate lower edge and the face plates of the connectors. On the wheel side of the joint, the jumper plate bottom edge pulls away from the face plate. On the opposite side the jumper plate lower edge bears against the face plate. Hence, the moment couple on the “opening” side of the joint is confined within the weld height (approximately 0.2 in. for a 1/4 in. weld) while the couple on the opposite side

extends from the bottom of the jumper plate to the top of the weld (about 0.8 in. for a 1/4 in. weld plus a 3/8 in. thick jumper plate) as indicated in Figure 26. If the moment applied to both sides is the same, the compressive stress on the "opening" side of the joint would be expected to be about four times the tensile stress on the opposite side of the joint. Keenan discounts this behavior, but comparison of the model with test results indicates that in almost all cases the interaction occurs as predicted by the model.

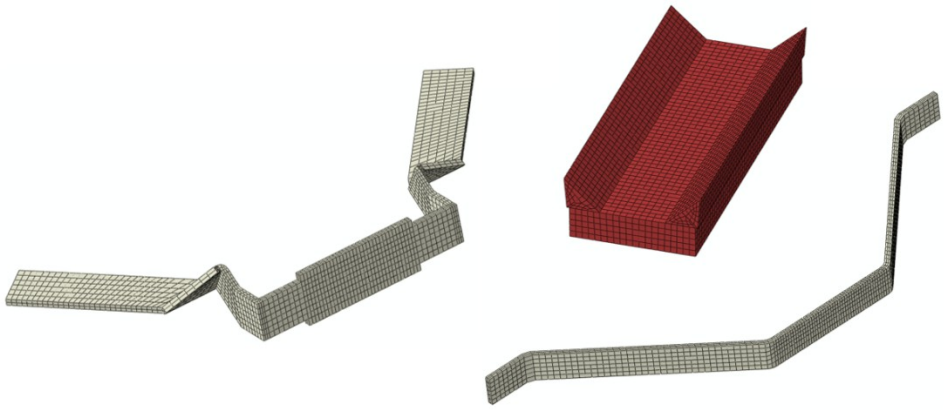

Figure 24: Finite element model meshing used for connection assemblies

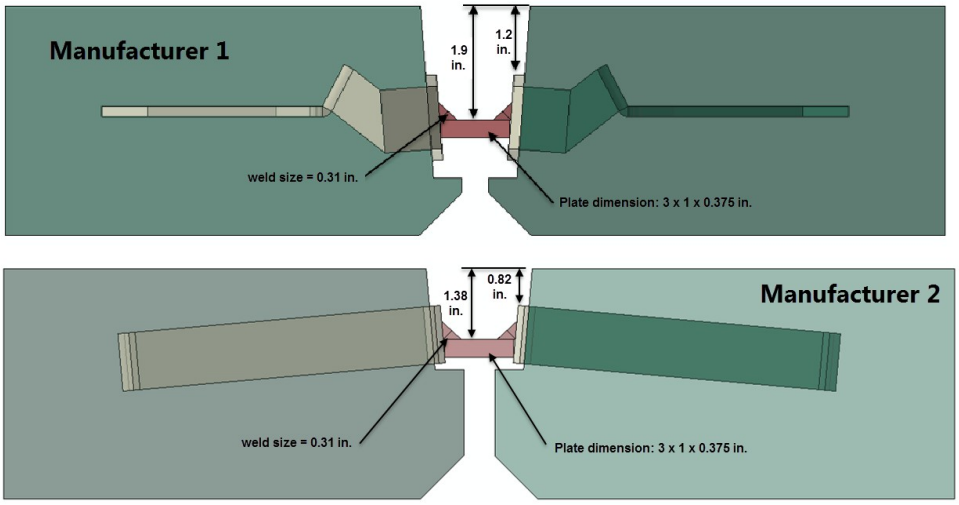

Figure 25: Connection assembly models and concrete flange edges showing dimension assumptions for the base model

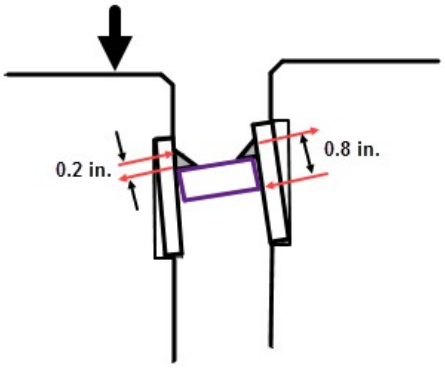

Figure 26: Postulated flange connection behavior

Refined Finite Element Model Results

The deformed shapes of the Manufacturer 1 and Manufacturer 2 FEA models are presented in Figure 27. Note that the model predicts the rotation of the face plates.

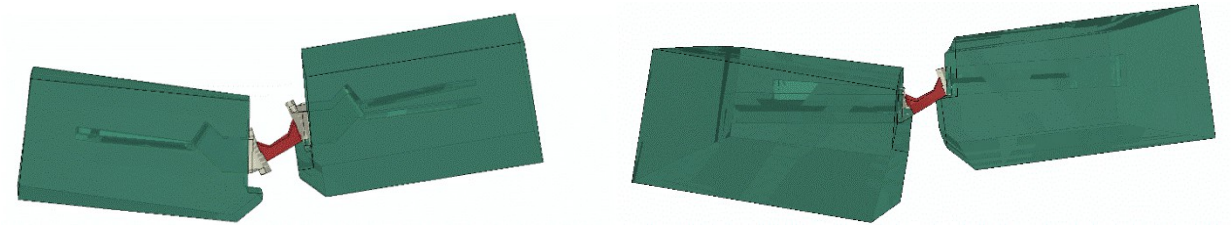

Figure 27: Manufacturer 1, left, and manufacturer 2, right, connection deformed shape under load (exaggerated 250X)

Differential displacement across the joints matched very well with the measured behavior as indicated in Figure 28. At a concentrated load of 1500 lbs. adjacent to a connector a differential vertical deflection of 0.005 in. is predicted.

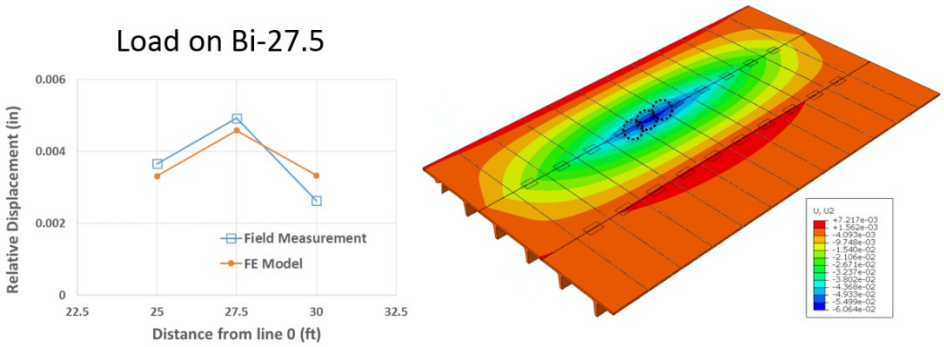

Figure 28: Differential displacement across DT flange joint, FEA prediction vs. field measurements

The main analysis result of interest is the stress measured at the root of the weld. This is an impossible location to measure, so comparisons are only possible at the faces of the welds. Weld stresses were found to vary with location along the sloped surface as well as along the length. Ranges of weld stresses predicted by the model at the approximate locations of the strain gages matched reasonably well (Figure 29). Previous modelling and hand calculations predict much higher stresses on the weld located on the

same side of the joint as the wheel load. This illustrates the inaccuracies provided by the preliminary analysis approach and the approach used by Keenan. The model also predicted a very low stress, both compressive and tensile, on the weld at the opposite side of the joint (Figure 30). The summation of these two stresses is the stress range imposed on the weld surface. The model predicts similar stress ranges at the weld root as the face of the weld.

The model predicted a range of compressive stresses along the face of the weld as shown in Figure 30. The average of these stresses was determined. Similarly, the average tensile stress on the opposite weld was calculated from the model results (Figure 30). The average tensile stress magnitude of 0.1 ksi is much less than one quarter of the compressive stress magnitude. The reason for this is believed to be a compression strut action acting through the jumper plate, which will be discussed later.

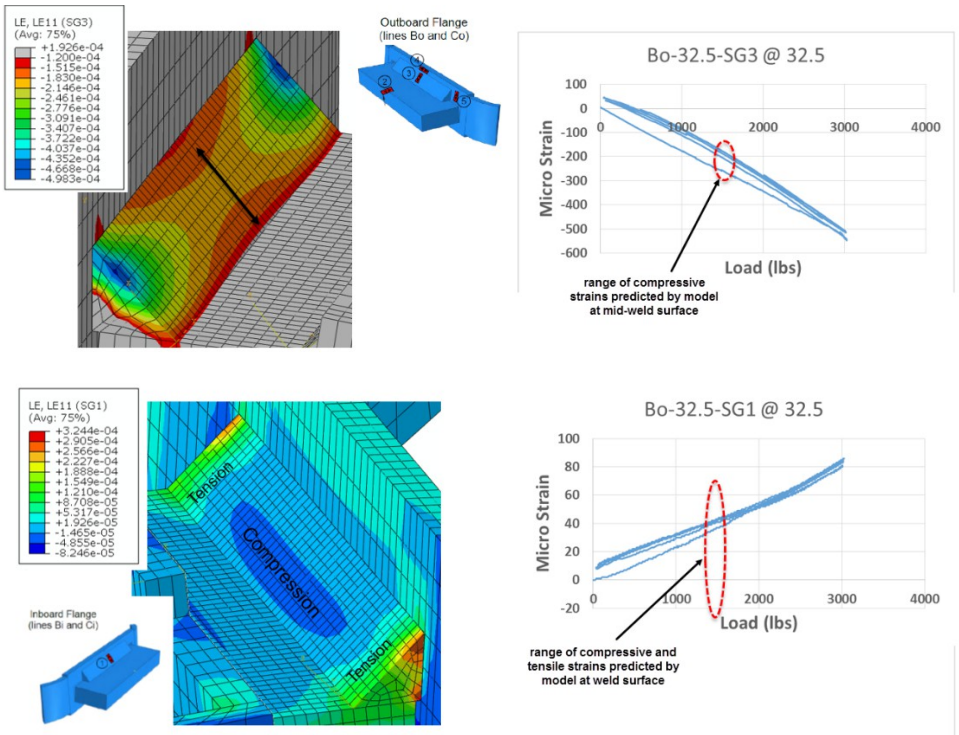

Figure 29: Strains measured on welds compared to calculated by the FEA model for 1500 lbs placed adjacent to the Bo-32.5 position

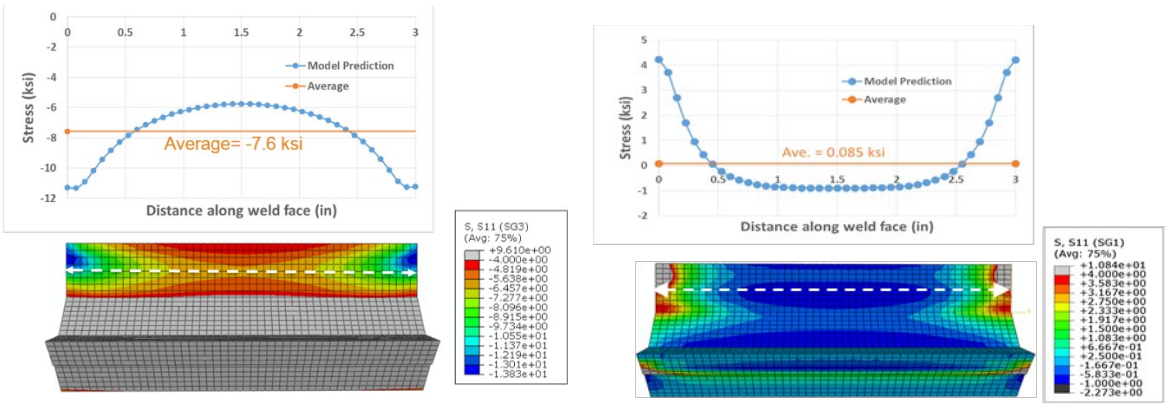

Figure 30: Variation in strains along mid-longitudinal axis of welds on both sides of the joint

With a working model that correlates reasonably well to test data, connection component dimensions could be varied and the effect that such variations have on the weld stresses could be evaluated. In Figure 31, the results of analyses are shown corresponding to five different weld sizes ranging from 0.19 in. to 0.50 in. A plot of average compressive weld stress versus the inverse square of weld size shows a linear relationship. Also varied were jumper plate widths and thicknesses. Plate widths studied were 0.75 in., 1.0 in., and 1.75 in. Plate thicknesses studied were 0.25 in. and 0.38 in. The variation in average weld compressive stress with plate width is presented in Figure 32. As is illustrated in the figure, average weld stresses vary linearly with plate width. Also shown in the figure are the shear and axial forces transferred across the jumper plate. The vertical shear forces are relatively constant 500 lbs. +/- 10% (i.e. approximately one third the applied load) regardless of plate or weld dimensions. The axial force however does vary significantly with plate width, with higher forces associated with greater plate widths. All forces are calculated at the midspan of the jumper plate, where the bending moment is at or near zero.

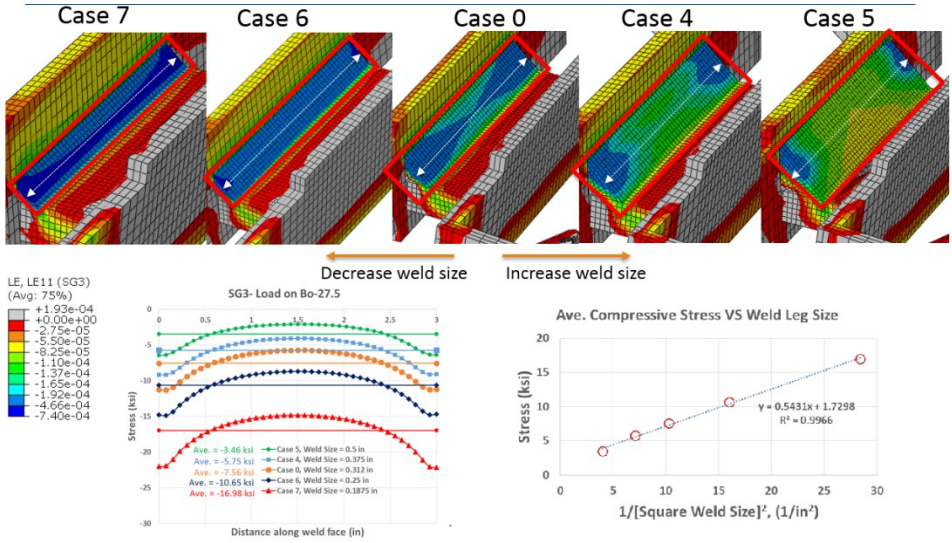

Figure 31: Variation in average compressive weld stress compared to weld leg size, Manufacturer 1 shown.

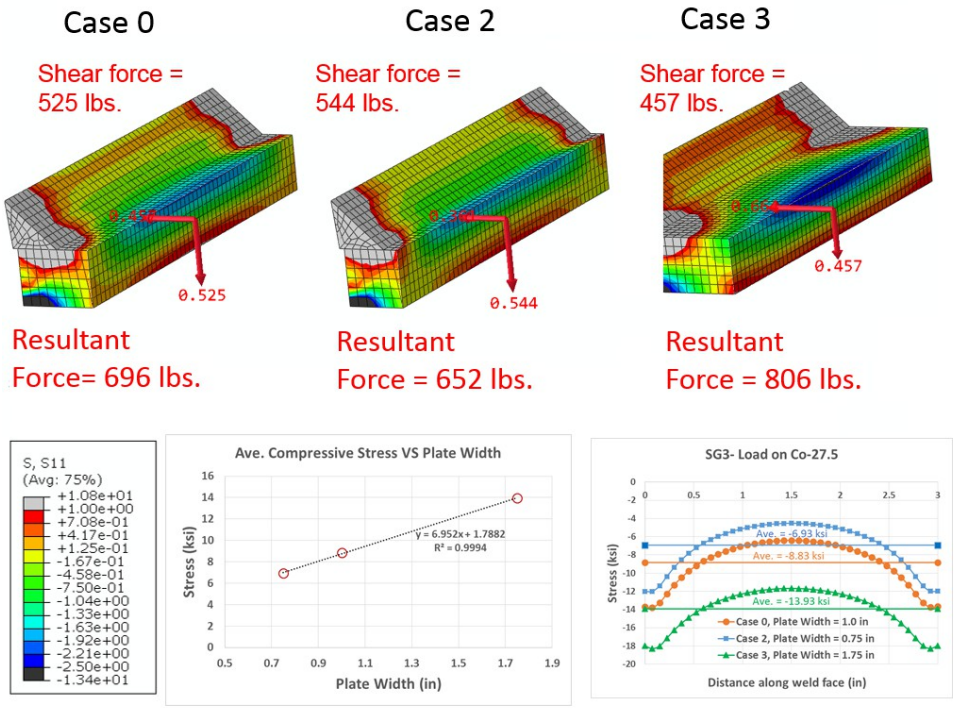

Figure 32: Variation in weld face compressive stress vs. plate width. Manufacturer 2 shown.

A comparison of variations in plate and weld dimensions and their effects on the weld stress ranges are summarized in Table 2. The predicted weld stress ranges for Manufacturer 2 were slightly higher than for Manufacturer 1. Varying the plate thickness was shown to have a minor influence on weld stresses.

Table 2: Comparison of stress ranges predicted by FEA for varying sizes of plates and welds

Case #	Weld size [in.]	Plate thickness [in.]	Plate width [in.]	Manufacturer 1, Stress range [ksi]	Manufacturer 2, Stress range [ksi]
0	0.31	0.38	1.00	7.7	9.8
1	0.31	0.25	1.00	8.3	9.7
2	0.31	0.38	0.75	5.9	7.5
3	0.31	0.38	1.75	12.4	15.8
4	0.38	0.38	1.00	5.8	6.8
5	0.50	0.38	1.00	3.7	3.8
6	0.25	0.38	1.00	11.5	13.3
7	0.19	0.38	1.00	18.5	20.0

Within the range of variables studied, weld face average stress ranges in psi were found to be approximately equal to P / 2000 x plate width/square of weld size, where P is the magnitude of the single concentrated load next to a connection in lbs. The average weld stress ranges predicted by the model (7.7 to 13.3 ksi) are typically higher than were measured (3.5 to 6.1 ksi). The reason for this is considered to be the weld size. The as-built weld sizes include a weld penetration into the base plate as was shown in

Lucier et al.. Considering the deeper penetration of the welds on the Manufacturer 2 connector compared to Manufacturer 1 helps explain the generally lower weld stresses measured for Manufacturer 2.

Simplified Approach for Determination of Connection Weld Stresses

Detailed three-dimensional finite element modeling provides the most comprehensive and accurate approach for determination of stress magnitudes in the connections. As shown in the previous section inclusion of all the floor components in the 3D model provides an accurate means of determination of the stresses. While this approach is accurate, the level of detail needed makes the method computationally time consuming for examining wide variations in connection details and floor configurations. An alternate approach is proposed for rapid assessment of stress levels in the connection weld. The approach consists of: (1) detailed finite element modeling of the connection; (2) utilization of the FE model to determine connection stiffness and weld stress level as a function of the shear force or displacement; (3) implementation of the connection stiffness as discrete springs in a simple shell model of the floor; (4) analysis of the shell model for a standard vehicle to determine maximum shear force in the connection of concern; (5) use the results from step 4 and 2 to determine maximum stress in the weld. To illustrate this approach, the results of the Lehigh tests and the NC State tests corresponding to Manufacturers 1 and 2 are studied.

Step 1: Simplified Finite Element Modeling of the Connection

These connectors were tested individually as noted previously and are initially modeled as single sided to verify the accuracy of the FE results. Based on observations of the elastic performance in the experiments the concrete remains undamaged under the loads of interest. Consequently, simplified boundary conditions are used in the model as opposed to detailed modeling of the concrete as detailed in Figure 33 and Figure 34. The assembly was modeled as the steel connector on elastic supports where the connector is embedded in the concrete. A rigid block was used to model the contact between the back of the connector face and the concrete. Nodal ties were used to join the weld to the connector face. In the downward load case, “hard” contact with no friction was used to model the contact between the slug and the connector face. Due to the relative simplicity of the model a fine mesh discretization can be used as illustrated in Figure 35. Connector modeling was conducted using ABAQUS version 6.13. All models were meshed with quadratic reduced integration brick elements (C3D20R). All material properties used in the model were linear elastic with a modulus of elasticity of 29,000 ksi and Poisson’s ration of 0.3.

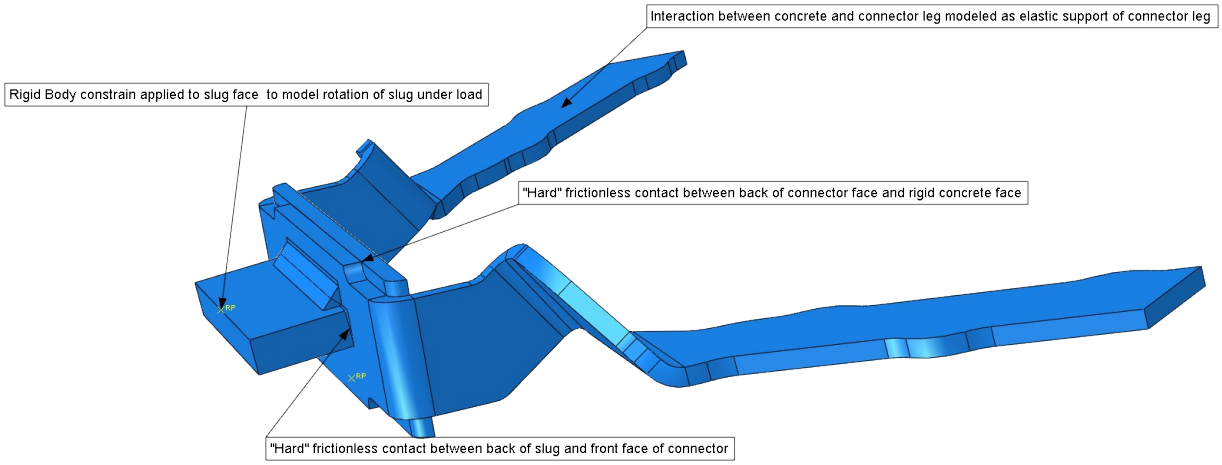

Figure 33: Single Sided Connector Model for Manufacturer 1

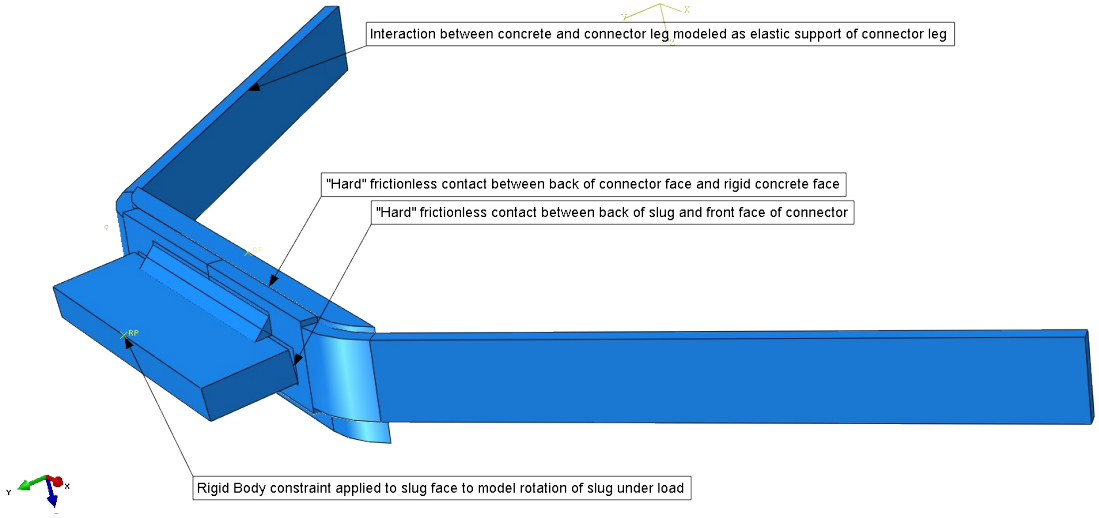

Figure 34: Single Sided Connector Model for Manufacturer 2

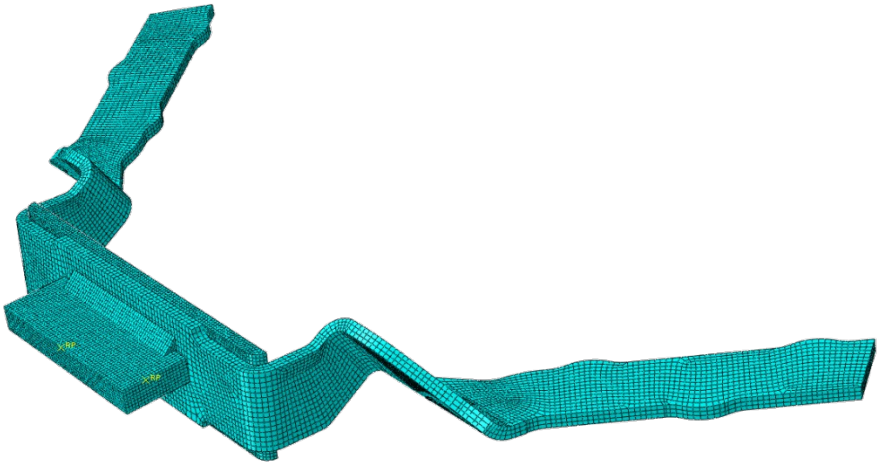

Figure 35: Meshed model (Manufacturer 1)

The connection assemblies were modeled with load in upward and load in downward direction to match that of the experimental program. The measured vertical force versus measured vertical deflection are

compared to the model results up to an applied vertical force of 525 lbs. The model shows good agreement for both Manufacturer 1 and 2 connectors as illustrated in Figure 36. The measured strains for strain gages 1, 2 and 3 versus measured vertical deflection are compared to the modeled values for vertical deflections between 0.012 and 0.016 in. (see Naito and Hendricks for more detail on gage location). These deflection values correspond to the point where the strain response becomes nonlinear in the test data, most likely due to rotation of the loading block and not due to any material non-linearity. The strain measurements are compared to the models in Figure 37 and Figure 38. In general, data from strain gages SG1, SG2, and SG3 compare well between the model and the test data. The accuracy of the model in computing both the global behavior and local strains validates the modeling approach.

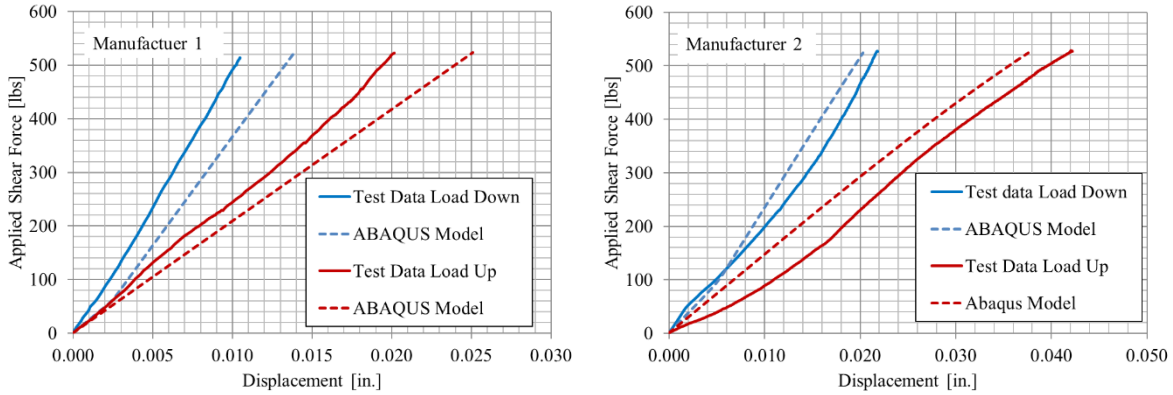

Figure 36: Comparison of numerical model with Naito and Hendricks load-displacement results for single sided loading, Manufacturers 1 and 2

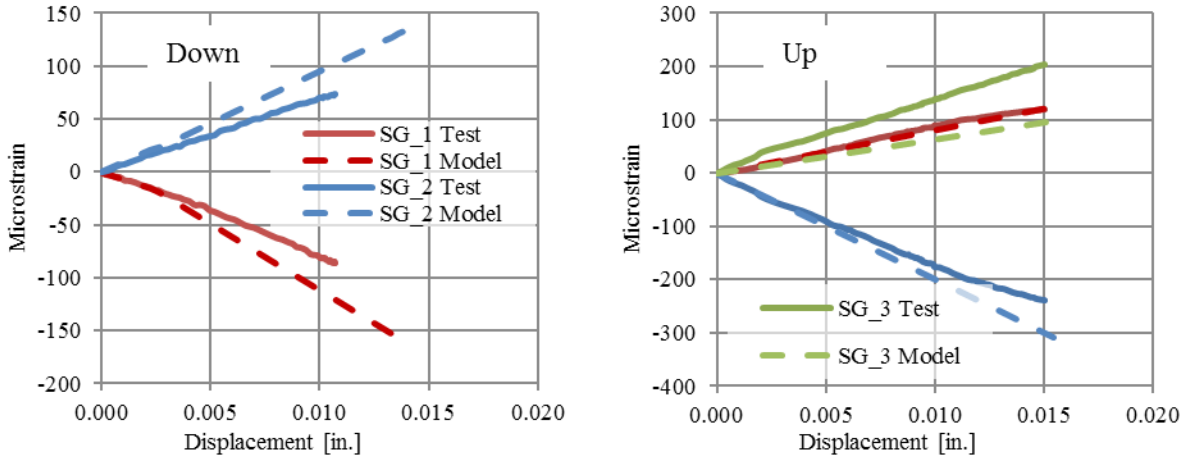

Figure 37: Comparison of numerical model with Naito and Hendricks strain-displacement results for single sided loading, Manufacturer 1

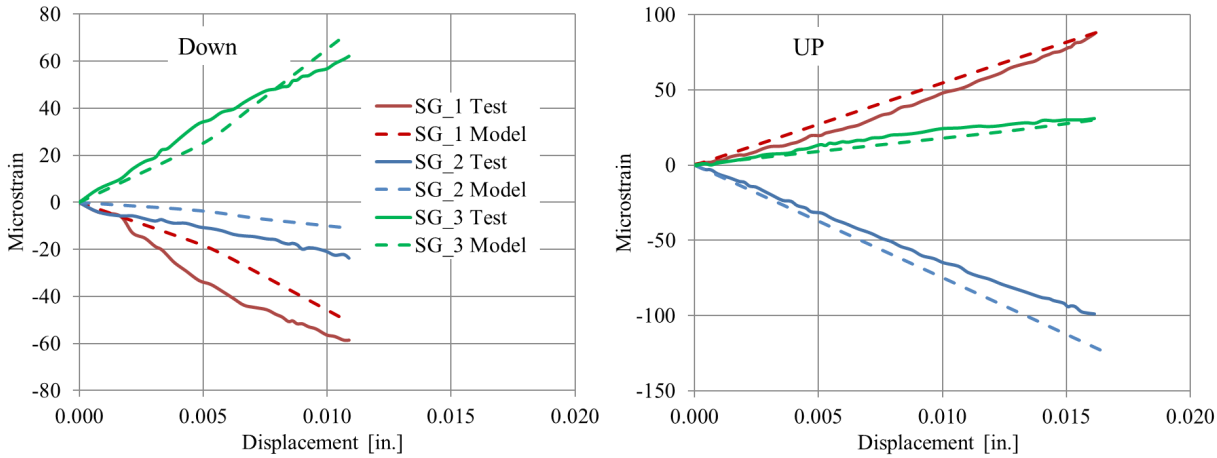

Figure 38: Comparison of numerical model with Naito and Hendricks strain-displacement results for single sided loading, Manufacturer 2

Step 2: Determination of Connection Stiffness

The FE models were extended from the single sided connection to the full flange to flange connection. The model was created by combining the upward and downward load models into a single assembly. The contact interactions between the two models were consistent with the single sided models. The connector legs on the "fixed" side were supported with the elastic support constraint as was done in the single sided assembly model. The load was applied as a vertical shear deflection of 0.01 in. applied to the "downside" connector at the point where the connector legs turn into the concrete. Only vertical deflection was allowed, all other deflections were held fixed. The force vs. deflection data from the combined assembly model was used to generate linear, uncoupled vertical shear stiffness for each connector type. The dimensions of the combined models were chosen to approximate the dimensions of the connections in the full scale test (Lucier et al.) and is illustrated in Figure 39 and Figure 40. The resulting stiffness of the connections are illustrated in Figure 41.

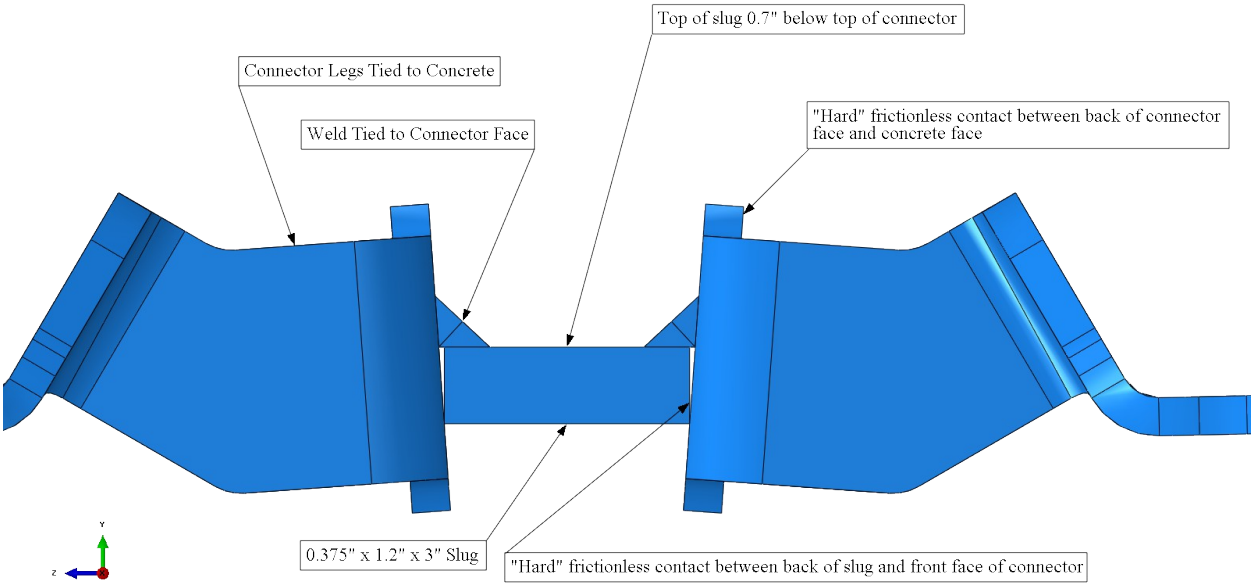

Figure 39: Details of Combined Assembly for Manufacturer 1

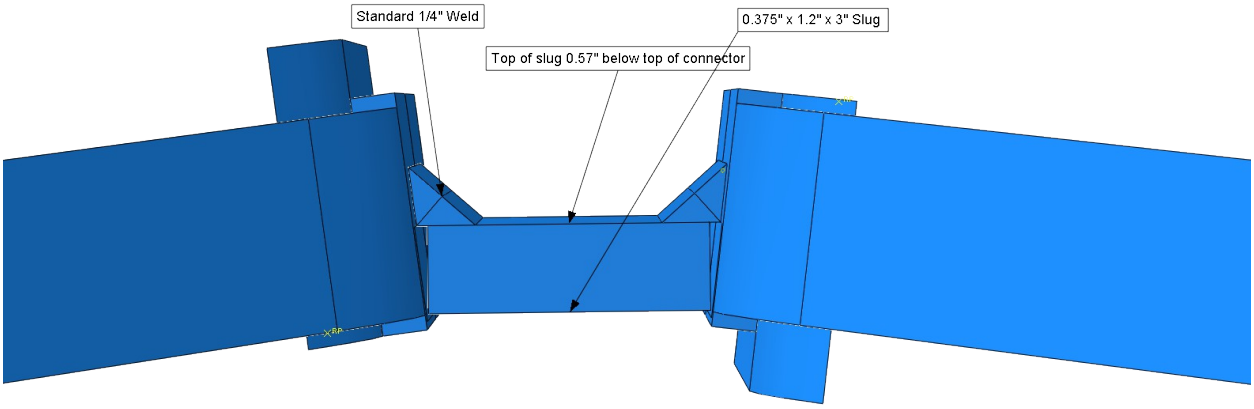

Figure 40: Details of Combined Assembly for Manufacturer 2

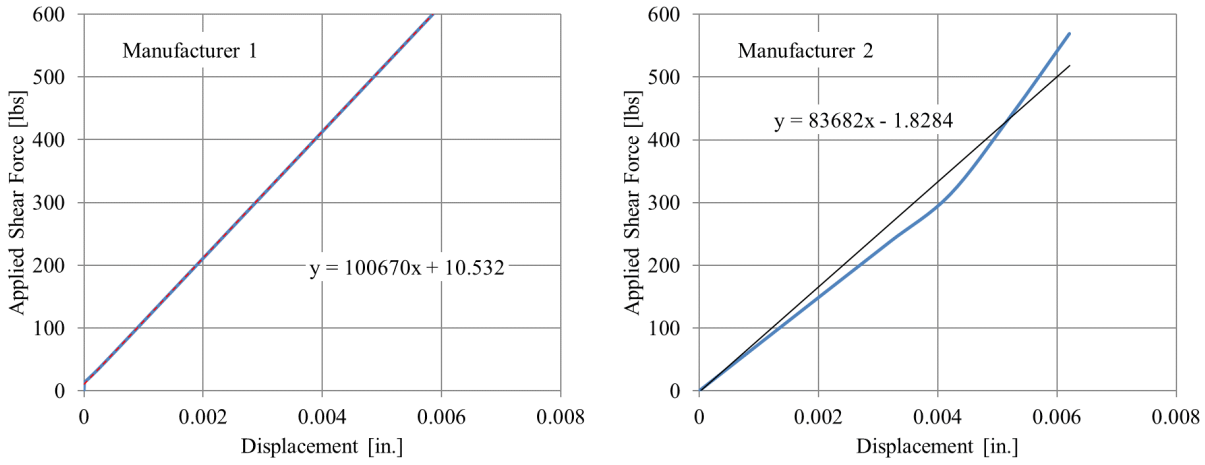

Figure 41: Estimated stiffness from finite element analysis

Step 3: Simplified Modeling of Double Tee Beam Deck

The linear vertical shear stiffness for each connector type was input as a vertical shear link in a SAP2000 shell element model of the NC State full size DT test setup (Lucier et al.). The shell element model of the NC State test setup was subjected to load cases T-Co-27.5, T-Ci-27.5, T-Bo-27.5, and T-Bi-27.5. The loads that were applied to the model were 1.5 kip at each load patch. A modulus of elasticity of 4,400 ksi and Poisson's ratio of 0.15 were used for the concrete in the NC State test model. The boundary conditions of the floor model included a longitudinal spring at bearing support with an axial stiffness of 107 kip/in. to match the restraints observed in the tests. The shell model is illustrated in Figure 42. An isometric view of the un-deformed (a) and deformed model (c – scale factor 500), and connection spring detail (b) is illustrated.

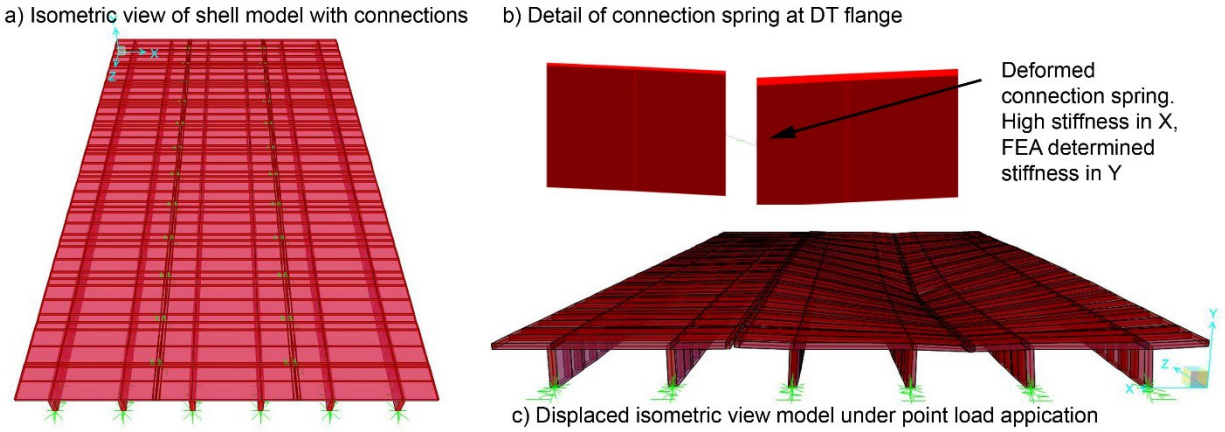

Figure 42: Overall View of SAP2000 shell/spring model

Step 4: Determine Shear Force and Relative Deflections in Connections

For each 1500 lb load case, the connection responses can be readily determined. The estimated shear forces and the differential deflection across the connection are summarized in Table 3. The estimated deflections across the joint are compared to three load cases. As noted, the measured deformations vary for the load cases. The deflections are approximated well by the model shell element model.

Table 3: Connector Forces and Differential Deflections from SAP2000 Model

Load Case	Estimated connector force at load point [lbs.]	Estimated differential deflection [in.]	Measured differential deflection for three load cases and (average) [in.]
27.5 Co	480	0.0050	0.002, 0.004, 0.006 (0.0040)
27.5 Ci	470	0.0060	0.002, 0.003, 0.002 (0.0023)
27.5 Bo	510	0.0050	0.001, 0.003, 0.002 (0.0020)
27.5 Bi	520	0.0040	0.006, 0.003, 0.005 (0.0047)

As an aside, this model can be readily modified to examine other deck configurations. A case study was conducted to examine the effect of DT size on the relative connection forces. A 1500 lb. point load was placed between the two connections closest to midspan. Three double tees were examined: 10DT34,

12DT30, and 15DT30. The connection spacing for each double tee matched that of the full scale tests (Lucier et al.). The relative DT sizes are shown in Figure 43 (left). As illustrated the connection force magnitude is most sensitive to local bending of the free edge of the flange, see Figure 43 (right). This conclusion is supported by the observation that as the moment of inertia increases from the 12DT30 to the 15DT30 the connection forces also increase. Furthermore, as the distance from the stem to the edge of the tee decreases from the 15DT30 to the 12DT30 and 10DT34 the local flange stiffness increases. This increase in local flange stiffness results in increased contribution from adjacent connections along the DT span. Further parametric studies can be readily conducted with this method.

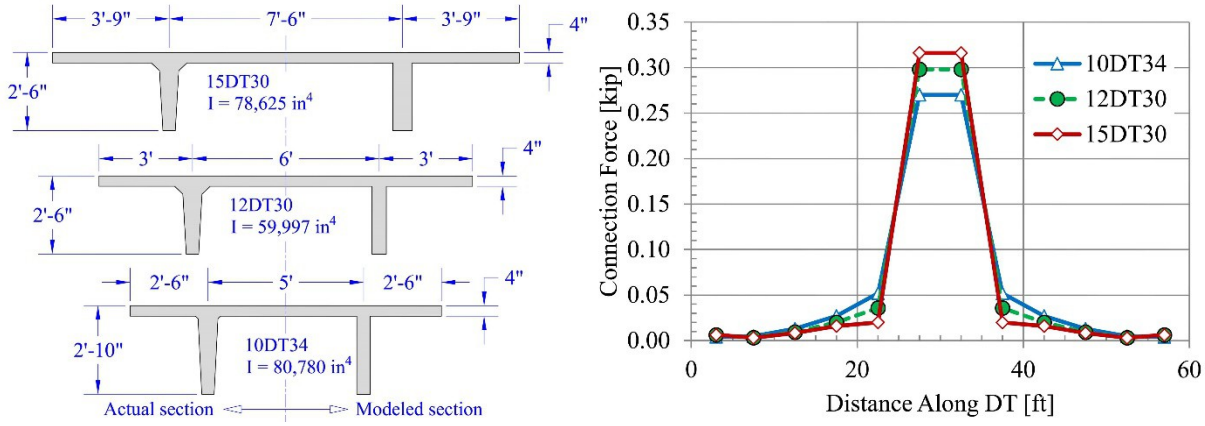

Figure 43: Connection force distribution for different DT sizes

Step 5: Use the Shell Model Results to Determine the Response of the Weld

The detailed finite element models of the connections can be used in conjunction with the differential deformations measured in the shell model to predict the stress and strain levels in the connection. Both the vertical deformation and the rotation history at the connection from the shell model were applied to the ABAQUS connection assembly model (Figure 44). The resulting strains from the ABAQUS model are compared to the strains measured during the Full Scale test to illustrate the accuracy of the approach.

The strain gages in the NC State test setup were typically located in regions where there was a large strain gradient, making strain comparisons difficult without knowing exactly where on the connector the gages were located. As previously shown, the stresses and strains vary considerably along the welds. A sample of the variation in maximum principal stresses in the detailed connection model are illustrated in Figure 44. This model can be used to determine the strain or stress at any location of interest in the connection. As an example, the strains from the ABAQUS connector model are compared to the measured strain values from the full scale test (Figure 45). The model data is taken as an envelope of the strains in the region where the strain gages were installed. In general, the measured strains fall within the envelope for gages SG-2, SG-4 and SG-5. Gages SG-1 and SG-3 were located on the face of the weld and are not

compared here due to the very large strain gradient on the face of the weld that was seen in the ABAQUS model. Dashed lines are model results and solid lines are test results

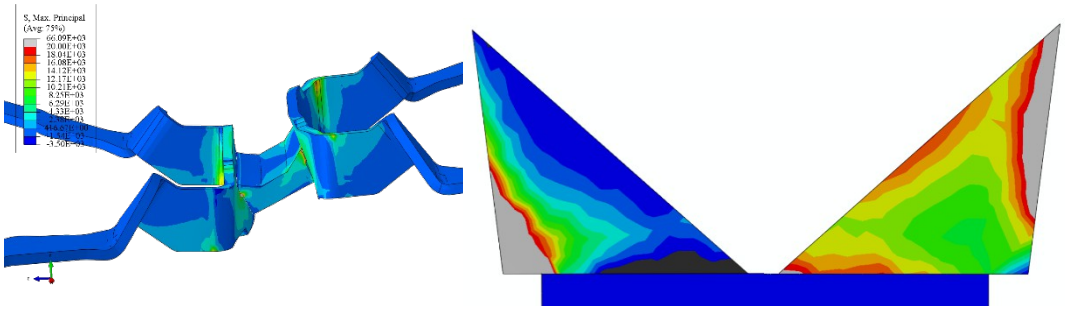

Figure 44: Variation in maximum principal stresses in welds

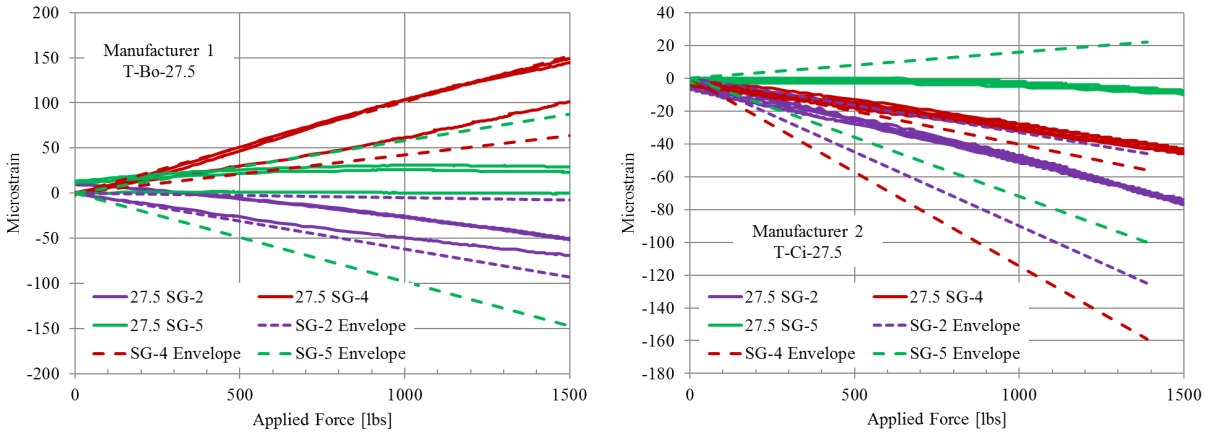

Figure 45: Comparison of connection strains from Lucier et al. with FE results

Analytical Prediction of Fatigue Strength

As illustrated in the preceding sections weld stresses cannot be computed using simple beam analogy models. Due to the flexibility of the boundary conditions and the configurations of traditional flange to flange connections the stresses vary considerably over the face and root of the welds. As discussed, these stresses can be accurately determined using either a comprehensive 3D finite element model of the diaphragm and all connections or a detailed 3D finite element model of the connection and a shell/spring model of the diaphragm. These tools however fall short of determining whether the connection is, in the end, susceptible to fatigue induced failure.

Research by Sorensen et al. examined the performance of fillet welds subject to varying degrees of bending. The study was specifically conducted to address details where the throat of the weld is subject to a combination of bending, shear and membrane action. This loading scenario is akin to the demands seen in a flange to flange fillet weld. Due to the complexity of the stress distribution in these connections and the indeterminacy of the problem the authors noted that a “desk-calculation-based” estimate of stress is not viable. As an alternate, finite element approaches are recommended for determination of the critical stress parameter used to assess fatigue life. Two fatigue stress parameters named SCF4 and SCF5 were

developed in their study for use in determination of fatigue life. The SCF4 stress parameter is based on "*linear extrapolation of the principal stress from two points in the fillet throat section to the weld root*." The SCF4 stress is obtained by extrapolating the maximum principal stresses at the quarter points on the weld throat section to the weld root. The SCF5 provides a better fit and is "*based on linear extrapolation of the six basic stress components in the fillet throat section to the weld root*."

Using this approach an SN curve for SCF4 was developed and is reproduced in Figure 46. The mean S-N curve is given by the formula:

Where:

< 5,000,000

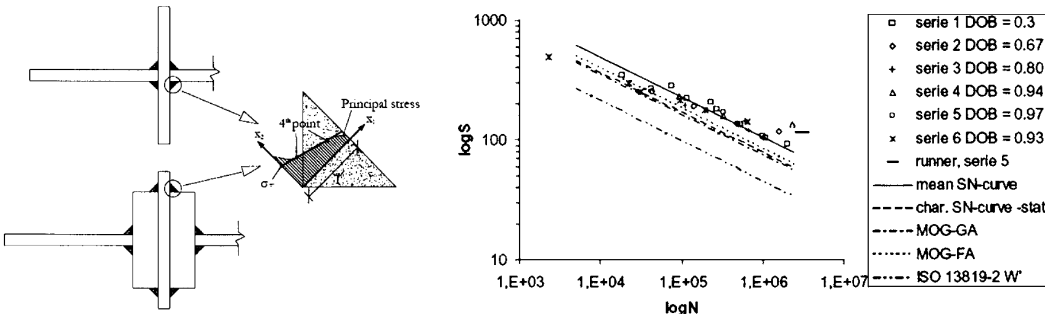

Figure 46: Weld detail [*Figure 12 - from Sorensen et al.*] and SCF4 Stress (in MPa) Parameter SN Curve [*Figure 14 - from Sorensen et al.*]

The SCF4/SCF5 approach was developed specifically for details commonly used in the offshore structure industry. The detail differs from that of flange to flange connections in that the base plate to which the weld is attached is much more rigid than that of a typical manufactured connection faceplate. With a rigid boundary condition the stress at the root of the weld would be constant along the length of the weld. This is much more severe than the cases observed in the previously shown analyses where the weld has a high stress at the ends and a relatively lower value over the majority of the length. Note that the lowest stress range sufficient to propagate a fatigue crack in Sorensen (see Figure 46) was about 100 MPa (14,500 psi). This is a significantly higher critical stress than assumed by Keenan.

Conclusions and Future Work

A comprehensive examination of flange to flange connections used for double tee connections in precast/prestressed concrete parking decks was conducted. The goal was to identify if the welded connections are susceptible to fatigue induced failures. The study included an informal survey of the industry, field measurements of differential connection deflection in existing parking structures, testing of

commonly available connections, testing of a full scale prototype deck, and extensive numerical modeling of the response. The research results indicate the following:

- Informal polls of producers who had been fabricating and erecting double tee parking garages for decades indicated that weld fractures were uncommon and when they occurred were usually associated with atypical joint conditions or lack of maintenance.
- Problems with flange to flange joints do occur on occasion, but are typically due to atypical joint conditions or a lack of maintenance.
- An evaluation of typical parking structures indicates that connection cycles could exceed 20 million cycles in 30 years but only for a select number of garages and selected locations within those garages. The majority of connections would be subject to much lower number of cycles.
- Observation of field measurements on existing parking structures indicate that relative displacements across the connection are small and are on the order of 0.005 to 0.015 in. for a typical vehicle load.
- Connection stiffness in the vertical direction varies based on the connection configuration. Finite element analysis and experimental testing of conventional connections indicates that the out of plane stiffness typically ranges from 30 to 110 kips/in.
- Detailed finite element analysis methods are shown to provide accurate estimations of both deflection, stiffness and local strains at the connection as verified by test.
- The FEA results show that the average stress levels in the fillet weld vary linearly to the inverse of the square of the weld size and also vary linearly with the jumper plate width.
- An alternative approach consisting of detailed FEA of the connection and a simple shell model of the floor deck shown to provide accurate estimate of connection response and can be used to examine other connections and floor configurations with less computational effort. This approach shows that the connection force magnitude is most sensitive to local bending of the free edge of the flange as opposed to the moment of inertia of the DT section.
- Initial work on estimation of fatigue life has been identified and work is progressing on using the approach for flange to flange connection evaluation.
- One case study is included in this paper where fatigue cracks were found. In that specific case, the weld was undersized (0.15 in. compared to 0.25 in.) and the plate width oversized (1.5 in. vs 1.0 in.). Using the relationships developed in this study, the case study welds would be expected to be

exposed to stresses four times greater than the stress associated with a connection with the specified dimensions.

The research results clearly indicate that the force transfer across a flange to flange connection as a result of vertical loads on the floor is complex. Stresses can be high in some cases but the occurrence of fatigue induced cracking is limited to a few instances. These cases, if they were to occur, would manifest at the middle of the double tee span where vehicles are most likely to pass. As shown in the study, the vehicle loads are resisted primarily by local flange flexure and the connections nearest the load point. Consequently, in the rare case that a fatigue induced failure were to occur it is unlikely that failures would propagate along the joint to other connectors outside the drive path. Furthermore, the integrity of the floor system to lateral earthquake and wind loads would be minimally impacted in the rare case of a fatigue induced failure. As shown, possible failures would be at the midspan leaving the connections at the ends of the double tee, especially the chord connection, intact to resist the required in plane shear and tension/compression forces. In other words, precast double tee parking structures are indeed safe against fatigue induced failure due to seismic events.

Acknowledgements

The authors would like to recognize that the experimental studies conducted as part of the research effort were funded by the Precast/Prestressed Concrete Institute. Connector hardware material was donated by manufacturers. Many individuals contributed to the research effort including: Roger Becker, Ned Cleland, Larbi Senour, Harry Gleich, Chuck Wynings, Chuck Magnesio, and Steven Altstadt.

References

1. ABAQUS (2016) `ABAQUS Documentation', Dassault Systèmes, Providence, RI, USA.

2. American Society of Civil Engineers. Minimum design loads for buildings and other structures. ASCE/SEI 7-10. American Society of Civil Engineers, 2013.

3. Aswad, A. (1977). “Comprehensive report on precast and prestressed connectors testing program.” Research Rep., Stanley Structures, Inc., Denver, CO.

4. Botros, A., Lucier, G., Rizkalla, S., Gleich, H., “Behavior of free and connected double-tee flanges reinforced with carbon-fiber reinforced polymer,” Journal of the Precast/Prestressed Concrete Institute, Sept.-Oct., 2016, pp. 49-68.

5. EPA, “Light-Duty Automotive Technology, Carbon Dioxide Emissions, and Fuel Economy Trends: 1975 Through 2013,” Trends Report, Report No. EPA-420-R-16-010, United States Environmental Protection Agency, November, 2016.

6. Keenan, L; “Analysis of Welded Precast Double-Tee Connection Failures Due to Cyclic Fatigue from Vehicular Loading”, presentation and handout at ICRI NE meeting on May 10, 2016.

7. Lucier, G., McEntire, J., Rizkalla, S., “Double-Tee Flanges Reinforced with CFRP Grid,” NC State University, Technical Report No. IS-12-20, June 2013.

8. Lucier, G., Nafadi, M., Naito, C., Rizkalla, S., Osborn, A., "Double Tee Flange Connections – Experimental Evaluation," 2017 PCI Conference Proceedings, Cleveland OH.

9. Naito, C., Cao, L., Peter, W., "Precast Double-Tee Floor Connectors Part I: Tension Performance," Journal of the Precast/Prestressed Concrete Institute, Vol. 54, No. 1, Winter, 2009, pp. 49-66.

10. Naito, C., Hendricks, R., "In-Plane and Out-Of-Plane Performance of the MC-Flange Connector," ATLSS Report No. 08-08, ATLSS Center, Lehigh University, September, 2008, 47 pages.

11. Naito, C., Hendricks, R., "Experimental Evaluation of Double Tee Flange Connectors Subject to Out-of-Plane Loading," ATLSS Report No. 16-07, ATLSS Center, Lehigh University, July, 2016, 71 pages.

12. Oliva, M. G. (2000). "Testing of the JVI flange connector for precast concrete double-tee systems." Test Rep., Structures and Materials Test Laboratory, Univ. of Wisconsin, Milwaukee.

13. PCI Industry Handbook Committee, "PCI Design Handbook Precast and Prestressed Concrete," 1st Edition, Precast/Prestressed Concrete Institute, Chicago, IL, 1971.

14. PCI Industry Handbook Committee, "PCI Design Handbook Precast and Prestressed Concrete," 2nd Edition, Precast/Prestressed Concrete Institute, Chicago, IL, 1978.

15. PCI Industry Handbook Committee, "PCI Design Handbook Precast and Prestressed Concrete," 3rd Edition, Precast/Prestressed Concrete Institute, Chicago, IL, 1985.

16. PCI Industry Handbook Committee, "PCI Design Handbook Precast and Prestressed Concrete," 4th Edition, Precast/Prestressed Concrete Institute, Chicago, IL, 1992.

17. PCI Industry Handbook Committee, "PCI Design Handbook Precast and Prestressed Concrete," 5th Edition, Precast/Prestressed Concrete Institute, Chicago, IL, 1998.

18. PCI Industry Handbook Committee, "PCI Design Handbook Precast and Prestressed Concrete," 6th Edition, Precast/Prestressed Concrete Institute, Chicago, IL, 2002.

19. PCI Industry Handbook Committee, "PCI Design Handbook Precast and Prestressed Concrete," 7th Edition, Precast/Prestressed Concrete Institute, Chicago, IL, 2010.

20. Pincheira, J. A., Oliva, M. G., and Kusumo-Rahardjo, F. I. (1998). "Tests on double flange connectors subjected to monotonic and cyclic loading." PCI J., 43(3).

21. Ren, R., Naito, C., "In-Plane and Out-Of-Plane Performance of the MC-Flange Connector – Series 2," ATLSS Report No. 10-02, ATLSS Center, Lehigh University, June, 2010, 40 pages.

22. Ren, R., Naito, C., "Precast Concrete Diaphragm Connector Performance Database," ASCE Journal of Structural Engineering, Vol.139, No.1, Jan., 2013, pp. 15-27. DOI: 10.1061/(ASCE)ST.1943-541X.0000598.

23. Shaikh, A. F., and Feile, E. P. (2002). "Testing of JVI vector connector." Test Rep., Structural Engineering Laboratory, Milwaukee.

24. Sorensen, John Dalsgaard, et al. *Fatigue Analysis of Load-Carrying Fillet Welds,* Journal of Offshore Mechanics and Artic Engineering, Vol. 128, February 2006.

25. Spencer, R. A., and Neille, D. S. (1976). "Cyclic tests of welded headed stud connectors." PCI J., 21(3), 70-83.

26. Venuti, W. J. (1970). "Diaphragm shear connectors between flanges of prestressed concrete T-beams." PCI J., 15(1), 67-78.

27. Wen, Y. K., & Yeo, G. L., "Design live loads for passenger cars parking garages". Journal of Structural Engineering, 127(3), 2001, pp.280-289.

28. Wilson, E. L., and A. Habibullah. "SAP2000 integrated finite element analysis and design of structures." Analysis reference. Computers and Structures (1997).

29. Wiss, Janney, Elstner Associates, Inc. (WJE). (2002). “Dayton/Richmond flange-to-flange connector tests.” Test Rep., WJE, Northbrook, IL.